

OPTIMIZATION OF OPERATING REGIMES OF PULSED ELECTRON-BEAM-  
CONTROLLED CO<sub>2</sub> LASERS

V. A. Danilychev, I. B. Kovsh,  
and V. A. Sobolev

UDC 621.378.33

The dependences of the lasing characteristics of the pulsed electron-beam-controlled CO<sub>2</sub> lasers on the excitation conditions are investigated. The dependences of the laser efficiency, of the emission pulse duration, and of the specific energy output on the duration and intensity of the pump, on the composition of the working gas mixture, and on the resonator parameters are analyzed. It is shown that the optimal pump-pulse duration needed to attain a high specific energy output and efficiency is 10-40 usec, and that in this case the best working mixtures are those containing CO<sub>2</sub> and N<sub>2</sub> in a ratio (1:2)-(1:4). Introduction of a small addition of H<sub>2</sub> into a CO<sub>2</sub>:N<sub>2</sub> mixture leads to an efficiency 15-20% higher than in analogous mixtures without the H<sub>2</sub>. When the CO<sub>2</sub>:N<sub>2</sub>:He mixture is replaced by CO<sub>2</sub>:N<sub>2</sub>:H<sub>2</sub>, the maximum efficiency realized in the experiment remains practically exchanged, but the specific energy output increases because a higher specific pump energy is reached.

One of the most important tasks in the development of an electron-beam-controlled laser (EBL) with specified output characteristics (power, energy, and spectral composition of the emission, divergence, efficiency) is to find its optimal working parameters, i.e., to determine the geometry of the active region, the composition and pressure of the working gas mixture, the characteristics of the resonator, as well as the values of the specific energy input, pump power, and field intensity in the discharge gap, at which the specified lasing characteristics of the EBL are realized with maximum reliability, stability, and effectiveness. The set of the indicated parameters determines almost uniquely the dimensions of the working chambers, the characteristics of the laser supply system (as well as the characteristics of the gas-flow system in the case of the cw or frequency-pulse regime), and consequently determines the dimension and the weight of the installation, its technical efficiency, and in final analysis its cost.

Detailed investigations of discharge and lasing characteristics of pulsed EBL using CO<sub>2</sub>:N<sub>2</sub>:He mixtures, at excitation pulse durations 10<sup>-7</sup>-10<sup>-6</sup> sec and (2-5)·10<sup>-5</sup> sec, were carried out in our earlier studies [1-5]. The data accumulated in these studies as well as the experimental results obtained in other laboratories under analogous pumping conditions of CO<sub>2</sub> EBL [6-11] make it possible to carry out at the present time the complete engineering design calculations for a pulsed electron-beam-controlled CO<sub>2</sub> laser intended to work in one of the indicated regimes [12]. However, in connection with the ever increasing need for pulsed and frequency-pulsed EB CO<sub>2</sub> lasers, which are widely used in various branches of science and technology, it became necessary to determine the optimal parameters of such lasers for a wide range of emission-pulse powers and durations, since these values differ for different applications. The only common requirement is that the parameters be reproducible from pulse to pulse and that the efficiency be as high as possible. In addition, since the newly developed installations should operate over a long time, the problem of the operating cost of the laser installation is of no little importance. To lower the operating costs it is necessary to dispense above all with the use of expensive helium as a component of the active medium. In principle, the operating characteristics of EB CO<sub>2</sub> lasers can be predicted by numerically simulating the laser operation, and appropriate procedures were developed in [13, 14]. The accuracy of these predictions, however, is insufficient for the choice of the operating regime of the installation, inasmuch as even the presently most complete numerical calcu-

---

Translated from Trudy Ordena Lenina Fizicheskogo Instituta im. P. N. Lebedeva Akademii Nauk SSSR, Vol. 116, pp. 98-117 (1980).

lations for pulsed EB CO<sub>2</sub> lasers are carried out for idealized conditions, wherein the reduced field intensity  $E/p$  is assumed optimal, the pumping is assumed perfectly uniform over the active volume, the gradients of the gas temperature and pressure in the active region are assumed to be zero during the time of the pump pulse, etc. Therefore, to corroborate the choice of the operating characteristics of pulsed EB CO<sub>2</sub> laser with specified output parameters, experimental research must be carried out in a wide range of laser excitation durations and intensities, all the more since under real conditions the possibility of reaching a particular operating regime of a pulsed EB CO<sub>2</sub> laser is frequently limited by such factors as the insufficient breakdown strength of the optical elements, the instability of the volume discharge in the active medium, the presence in the working gases of impurities that alter the relaxation times of the excited molecules, etc. [4].

The present paper is devoted to an investigation of the dependence of the lasing characteristics of a pulsed CO<sub>2</sub> EBL on the excitation conditions. We analyze the dependences of the laser efficiency, of the emission-pulse duration, and of the specific energy output on the duration and intensity of the pump, on the resonator parameters, and on the composition of the working gas mixture. Particular attention is paid to operation of EB CO<sub>2</sub> lasers using gas mixtures in which helium is replaced by hydrogen. The data obtained in this paper make it possible to choose the optimal operating regimes of pulsed and frequency-pulsed EB CO<sub>2</sub> lasers with account taken of the restrictions imposed by the capabilities of contemporary electron guns and by the breakdown strength of the available optical elements.

## I. ENERGY AND TEMPORAL CHARACTERISTICS OF EB CO<sub>2</sub> LASERS AT VARIOUS DURATIONS AND INTENSITIES OF EXCITATION

### I.1. Experimental Setup and Measurement Procedure

The experiments were performed with a setup that made it possible to excite, by the electron-beam discharge method, up to 10 liters ( $10 \times 10 \times 100$  cm) of a working gas mixture [5]. The gas was ionized with an electron gun having a directly heated thermionic cathode. The beam was extracted into the discharge gap through a window covered with a thin foil in the plate separating the laser chamber from the electron-gun chamber. The transmission of the window for the electron beam was 50%, the beam cross section was  $10 \times 100$  cm, the energy of the fast electrons entering the discharge gap was 100 keV. By regulating the cathode heater, we were able to vary smoothly the current density of the electron beam entering the gas, from  $1 \mu\text{A}/\text{cm}^2$  to  $1 \text{mA}/\text{cm}^2$ . The electron gun was fed from a three-stage pulsed-voltage Marx generator (PVG) made up of IK-100/0.4 capacitors. The heating voltage was applied to the cathode through a 2-kW transformer with 200-kV high-voltage decoupling between the secondary and the primary windings. The power supply for the main discharge in the laser chamber was a bank of IK-50/3 capacitors. "Cutoff" of the electron-beam current was with the aid of a trigatron that shunted the electron-gun circuits. Starting pulses were applied from single-pulse generators to the trigatron that switched the PVG circuit and to the cutoff trigatron. A delay system, made up of two G5-15 oscillators, made it possible to regulate smoothly the time interval between the turning-on of the PVG and the cutoff of the electron-gun cathode voltage in the range from  $\sim 3$   $\mu\text{sec}$  to  $\sim 1$  msec, and to vary correspondingly the duration of the ionization pulse of the working gas mixture. The rise time of the electron-beam pulse was in this case 1-1.5  $\mu\text{sec}$ , and the drop of the voltage of the electron-gun cathode over a time  $\lesssim 1$  msec did not exceed 30% (Fig. 1).

During the course of the experiments, we measured the following: the voltage on the cathode of the electron gun ( $U_e$ ), the voltage on the anode of the laser chamber ( $U_d$ ), the discharge current ( $I_d$ ), and the emission-pulse parameters. The dependence of the electron-beam current density ( $j_e$ ) on the heater power was plotted before the start of the laser experiments, in which the anode of the discharge gap was used as the fast-electron collector.

The waveform of the laser emission pulse was registered with a cooled Ge:Au photoresistor (resolution  $\sim 5 \cdot 10^{-7}$  sec), and the radiation energy was measured with a thermocouple calorimeter developed by the Experimental Design Office of the Lebedev Institute. The input aperture of the calorimeter was 70 mm and the calibration accuracy was 10%.

The measurement sequence for each of the investigated gas mixtures was the following. The time dependences of the discharge current and of the discharge-gap voltage were first plotted for several values of the initial voltage  $U_0$  on the capacitor bank (the oscillograms

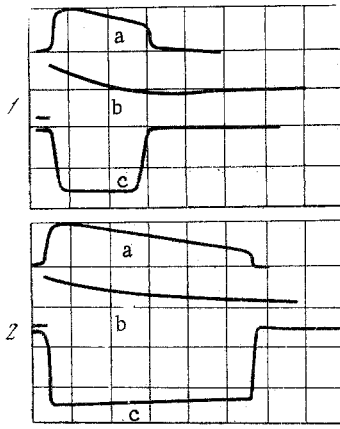


Fig. 1

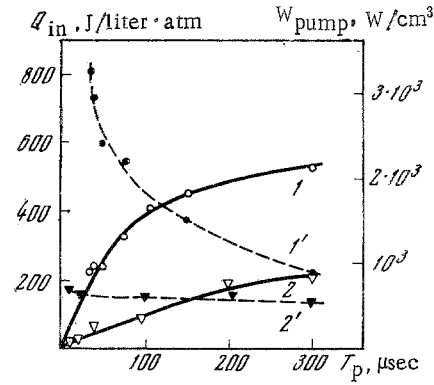


Fig. 2

Fig. 1. Oscillograms of the pulses of the discharge current (a) and of the voltages on the laser-chamber anode (b) and on the electron-gun cathode (c); sweep 20 μsec/div: 1) mixture CO<sub>2</sub>:N<sub>2</sub> (1:19), U<sub>0</sub> = 12 kV, j<sub>e</sub> = 0.8 mA/cm<sup>2</sup>; 2) mixture CO<sub>2</sub>:N<sub>2</sub>:He (1:2:3), U<sub>0</sub> = 9 kV, j<sub>e</sub> = 0.2 mA/cm<sup>2</sup>, p = 0.5 atm.

Fig. 2. Specific energy input and specific pump power vs pump-pulse duration at constant j<sub>e</sub>: 1, 1') mixture CO<sub>2</sub>:N<sub>2</sub> (1:2), p = 0.5 atm, U<sub>0</sub> = 20 kV, j<sub>e</sub> = 0.7 mA/cm<sup>2</sup>; 2, 2') mixture CO<sub>2</sub>:N<sub>2</sub> (1:19), p = 0.75 atm, U<sub>0</sub> = 20 kV, j<sub>e</sub> = 50 μA/cm<sup>2</sup>.

were registered alternately with an SI-17 two-beam oscilloscope, and the reference was the voltage pulse on the cathode of the electron gun). A comparison of the measured U<sub>d</sub>(t) and I<sub>d</sub>(t) plots with the calculated ones [15] made it possible to determine the electron-recombination coefficient b, the electron mobility μ, and the equilibrium electron density n<sub>e</sub> for the investigated mixture (the values of the cross section S and of the height d of the discharge gap, as well as the capacitance of the bank C and the duration of the ionization pulse T<sub>p</sub> were known). We measured next in the laser experiments the emission energy Q<sub>em</sub> and the residual value of the voltage U<sub>cap</sub> on the capacitor bank for different values of U<sub>0</sub> and registered simultaneously the waveforms of the emission pulses and of the voltage on the electron-gun cathode. The energy fed into the active medium during the time up to the termination of the lasing pulse was calculated from the formula [15]:

$$Q_{\text{pump}} = \frac{CU_0^2}{2} \left\{ 1 - [\text{ch}(n_p b T_{\text{em}})]^{-\frac{2\mu e S}{b C d}} \right\}, \quad (1)$$

and the average of the pump power during this time was defined as

$$W_{\text{pump}} = Q_{\text{pump}} / T_{\text{em}},$$

while the total energy input during the pump pulse Q<sub>in</sub> was determined from the known values of the initial and final voltage on the capacitor bank. Control experiments have shown that the calculated values of Q<sub>pump</sub> and W<sub>pump</sub> agree within the limits of the measurement error (~20%) with the values Q<sub>pump</sub> and W<sub>pump</sub> determined directly from the oscillograms of U<sub>d</sub> and I<sub>d</sub>.

To ensure high homogeneity of the ionization of the working gas, the distance between the anode and the cathode of the discharge gap was decreased to 7 cm, and the pressure in the active region was maintained in most experiments at 0.5 atm.

## I.2. Dependence of the Pump-Pulse Parameters on the Excitation Conditions

Typical oscillograms of the voltage pulses on the electron-gun cathode and in the dis-

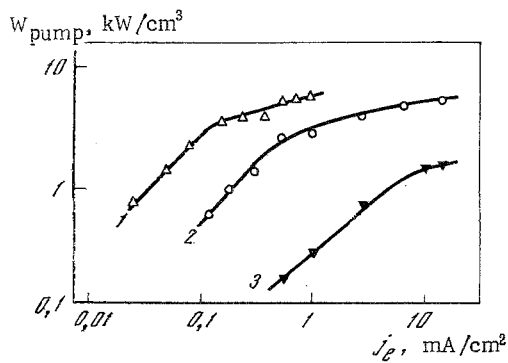


Fig. 3

Fig. 3. Specific pump power vs current density in electron beam: 1) mixture  $\text{CO}_2:\text{N}_2$  (1:19),  $p = 0.75$  atm,  $T_p = 20$   $\mu\text{sec}$ ,  $E/p = 3.2$   $\text{kV}/\text{cm}\cdot\text{atm}$ ; 2) mixture  $\text{CO}_2:\text{N}_2$  (1:4),  $p = 0.5$  atm,  $T_p = 45$   $\mu\text{sec}$ ,  $E/p = 2.2$   $\text{kV}/\text{cm}\cdot\text{atm}$ ; 3) mixture  $\text{CO}_2:\text{N}_2$  (1:2)  $p = 0.5$  atm,  $T_p = 20$   $\mu\text{sec}$ ,  $E/p = 4.4$   $\text{kV}/\text{cm}\cdot\text{atm}$ .

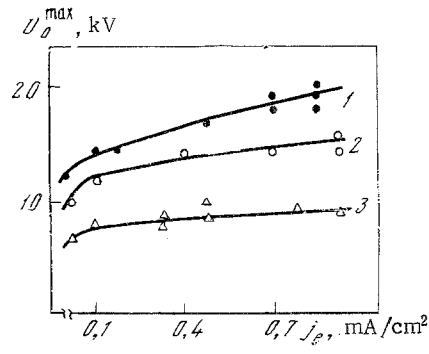


Fig. 4

Fig. 4. Dependence of the maximum permissible value of the initial voltage on the discharge gap on the current density in the electron beam. 1) mixture  $\text{CO}_2:\text{N}_2$  (1:9),  $T_p = 50$   $\mu\text{sec}$ ,  $C = 12$   $\mu\text{F}$ ; 2) mixture  $\text{CO}_2:\text{N}_2:\text{He}$  (1:4:5),  $T_p = 100$   $\mu\text{sec}$ ,  $C = 12$   $\mu\text{F}$ ; 3) mixture  $\text{CO}_2:\text{N}_2:\text{He}$  (1:1:8),  $T_p = 400$   $\mu\text{sec}$ ,  $C = 18$   $\mu\text{F}$ ;  $p = 0.5$  atm.

charge-current pulse are shown in Fig. 1. The measurements have shown that for the commercial purity gases used in the experiment, the coefficient of the electron-ion recombination at  $E/p \approx 3-5$   $\text{kV}/\text{cm}\cdot\text{atm}$  amounted to  $\sim 8 \cdot 10^{-7} - 10^{-6}$   $\text{cm}^3/\text{sec}$  for  $\text{CO}_2:\text{N}_2$  mixtures and  $(2-5) \cdot 10^{-7}$  for  $\text{CO}_2:\text{N}_2:\text{He}$  mixtures. The mobility of the electrons was 1.2-1.3 times higher than expected from the measurements [16] and calculations [17] performed for pure gases. The electron densities in the active region, calculated from the discharge-current oscillograms and from the energy characteristics of the discharge, turned out to be  $\approx 20\%$  larger than those predicted from the measured values of the current density  $j_e$  in the fast-electron beam. The causes of this effect are most readily the reflection of the fast electrons from the anode, which leads to "additional" ionization of the gases in the discharge gap [18], and the "focusing" of the beam on the anode in the presence of an electric field in the discharge gap [9].

Typical plots of the specific energy input and of the specific pump power averaged over the ionization pulse versus duration of the ionization pulse and versus the current density in the electron beam are shown in Figs. 2 and 3. At low current densities in the electron beam, the discharge proceeds in the electron-attachment regime and the pump power increases in proportion to  $j_e$ . When the ionization intensity, and hence the equilibrium density, is increased the discharge goes over into the recombination regime and  $W_{\text{pump}} \sim \sqrt{j_e}$ . The limiting value of  $j_e$  at which the discharge regime changes increases with increasing  $\text{CO}_2$  content in the mixture (Fig. 3). In the investigated range of field intensities (2-5  $\text{kV}/\text{cm}\cdot\text{atm}$ ) the attachment of the electrons to the  $\text{CO}_2$  molecules themselves is negligibly small [16], and consequently the experimentally observed attachment takes place with participation of other particles that are produced in the discharge with participation of  $\text{CO}_2$ . These particles are apparently  $\text{O}$ ,  $\text{O}_2$ ,  $\text{NO}$ ,  $\text{NO}_2$ , and  $\text{N}_2\text{O}$ . We note that at high density of the electrons an appreciable part of the energy enters the active medium already after the end of the ionization pulse — on the recombination "tail" of the current pulse. This energy becomes small compared with the energy input during the time  $T_p$  at  $T_p \geq 20$   $\mu\text{sec}$ , and at  $T \geq 50$   $\mu\text{sec}$  it can be neglected under the experimental conditions.

At low pump powers, the discharge becomes unstable under the experimental conditions. For example, in  $\text{CO}_2:\text{N}_2:\text{He}$  mixtures containing 50% helium, at field intensities  $E/p \approx 3$   $\text{kV}/\text{cm}\cdot\text{atm}$  and at current densities in the electron beam  $j_e \lesssim 0.1$   $\text{mA}/\text{cm}^2$  (this corresponded to an electron density in the active medium  $n_e \lesssim 10^{11}$   $\text{cm}^{-3}$ ), streamer breakdown set in already at 100-200  $\mu\text{sec}$  after the start of the ionization pulse. The same effect was observed in  $\text{CO}_2:\text{N}_2$  mixtures at  $E/p \approx 4-5$   $\text{kV}/\text{cm}\cdot\text{atm}$ . With increasing ionization intensity, the maximum permissible initial voltage ( $U_0^{\text{max}}$ ) on the discharge gap increases somewhat (inasmuch as at

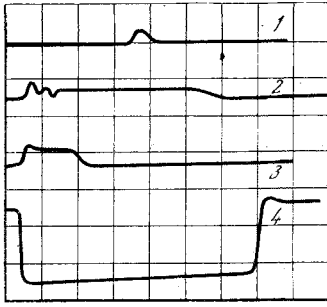


Fig. 5

Fig. 5. Emission pulses produced by excitation of the mixture  $\text{CO}_2:\text{N}_2:\text{He}$  (1:4:5),  $p = 0.5$  atm,  $T_{\text{out}} = 7\%$ ,  $U_0 = 12$  kV, sweep  $20 \mu\text{sec}/\text{div}$ : 1)  $j_e = 50 \mu\text{A}/\text{cm}^2$ ; 2)  $0.22 \text{ mA}/\text{cm}^2$ ; 3)  $0.9 \text{ mA}/\text{cm}^2$ ; 4) electron-gun cathode voltage.

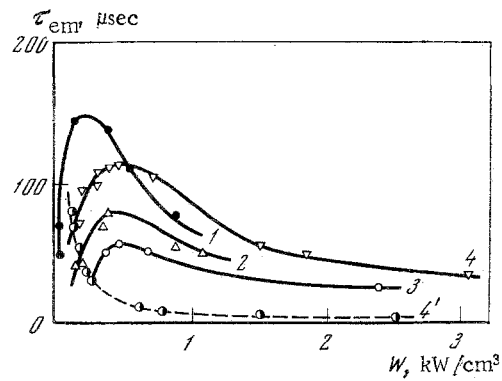


Fig. 6

Fig. 6. Dependence of emission pulse duration (1-3) and of the lasing delay time (4) on the specific pump power ( $p = 0.5$  atm): 1) mixture  $\text{CO}_2:\text{N}_2:\text{He}$  (1:4:5),  $T_{\text{out}} = 7\%$ ,  $E/p = 2-3 \text{ kV}/\text{cm}\cdot\text{atm}$ ; 2) mixture  $\text{CO}_2:\text{N}_2:\text{He}$  (1:2:3),  $T_{\text{out}} = 50\%$ ,  $E/p = 2-3 \text{ kV}/\text{cm}\cdot\text{atm}$ ; 3) mixture  $\text{CO}_2:\text{N}_2$  (1:19),  $T_{\text{out}} = 50\%$ ,  $E/p = 3-4 \text{ kV}/\text{cm}\cdot\text{atm}$ ; 4) mixture  $\text{CO}_2:\text{N}_2$  (1:4),  $T_{\text{out}} = 65\%$ ,  $E/p = 3-4 \text{ kV}/\text{cm}\cdot\text{atm}$ .

higher  $U_d$  the capacitor bank manages to become discharged more strongly within a time  $T_p$ ), see Fig. 4, and at  $j_e \lesssim 50 \mu\text{A}/\text{cm}^2$  the value of  $U_0^{\text{max}}$  decreases sharply. It is this which determined under the experimental conditions the maximum pump power of the laser. The lowest pump power at which a discharge existed for  $\gtrsim 50 \mu\text{sec}$  in fields sufficient to attain lasing, at  $p = 0.5$  atm, was  $\sim 100 \text{ W}/\text{cm}^3$ . We note that the limiting values of  $U_d$  and  $E/p$  at which the volume discharge is stopped turn out to be connected by the relation

$$[n_e(E/p)^2]_{\text{lim}} \simeq \text{const}(p, d),$$

which agrees well with the results obtained in [15].

### I.3. Dependence of the Energy and Temporal Characteristics

#### of an EB $\text{CO}_2$ Laser on the Excitation Intensity

The experiments were performed with hemispherical resonators of varying  $Q$ . The "total reflector" was a convex polished copper mirror with curvature radius 10 m. The radiation was extracted through dielectric interference output mirrors on NaCl substrates with different transmission coefficients  $T_{\text{out}}$ . The dielectric strength of multilayer dielectric mirrors is low and furthermore decreases rapidly with increasing number of layers [3], and when pure substrates of high dielectric strength are used lasing can be reached only with intense excitation, which cannot be realized in the regime of long ( $\gtrsim 50 \mu\text{sec}$ ) pump pulses because of the instability of the discharge [4]. Therefore, investigations of the lasing characteristics of EB  $\text{CO}_2$  lasers were carried out in the present study under pump conditions  $W_{\text{pump}} \lesssim 2-3 \text{ kW}/\text{cm}^3$ , for which the radiation fluxes at the output mirrors with  $T_{\text{out}} = 10-50\%$  did not exceed the mirror damage threshold. Typical oscillograms of laser-emission pulses are shown in Fig. 5. Owing to the insufficient temporal resolution of the employed radiation detector, the characteristic spike due to the turning on of the gain is weakly manifest on the oscillograms even at high pump powers.

At a constant pump-pulse duration, with increasing excitation intensity (this increase was produced in the experiments by increasing the current density in the fast-electron beam at a constant initial voltage on the capacitor bank), the delay of the emission pulse relative to the start of the pump decreases from  $\tau_{\text{del}} \approx T_p$  to  $\tau_{\text{del}} \ll T_p$ , and the lasing duration first increases rapidly, reaches a certain maximum value, after which it begins to decrease monotonically (Figs. 5 and 6). A maximum emission pulse duration corresponded to

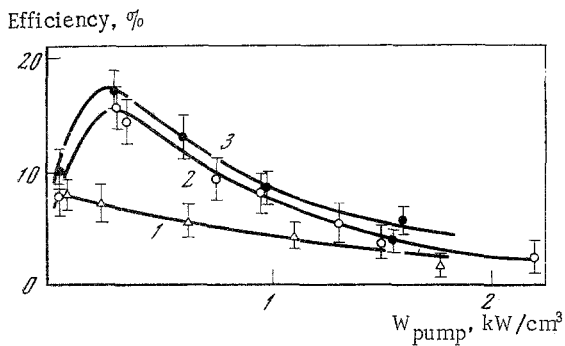


Fig. 7

Fig. 7. Dependence of the "effective" laser efficiency on the pump power averaged over the emission-pulse time ( $p = 0.5$  atm,  $T_p = 200$   $\mu$ sec): 1) mixture  $\text{CO}_2:\text{N}_2:\text{He}$  (1:1:8),  $T_{\text{out}} = 7\%$ ,  $E/p = 2.5$  kV/cm $\cdot$ atm; 2) mixture  $\text{CO}_2:\text{N}_2$  (1:4),  $T_{\text{out}} = 50\%$ ,  $E/p = 4$  kV/cm $\cdot$ atm; 3) mixture  $\text{CO}_2:\text{N}_2$  (1:2),  $T_{\text{out}} = 50\%$ ,  $E/p = 4$  kV/cm $\cdot$ atm.

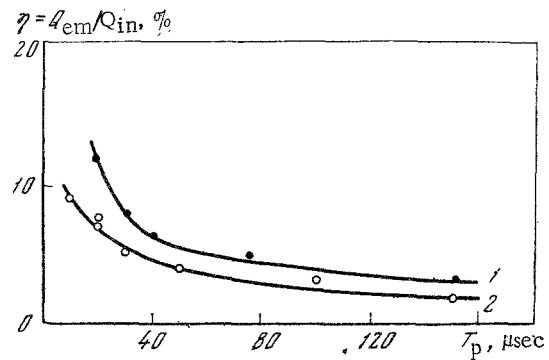


Fig. 8

Fig. 8. Dependence of the total efficiency on the pump-pulse duration ( $p = 0.5$  atm,  $T_{\text{out}} = 50\%$ ,  $E/p = 4-5$  kV/cm $\cdot$ atm): 1) mixture  $\text{CO}_2:\text{N}_2$  (1:2),  $U_0 = 20$  kV,  $j_e = 0.7$  mA/cm $^2$ , 2) mixture  $\text{CO}_2:\text{N}_2$  (1:4),  $U_0 = 19$  kV,  $j_e = 0.6$  mA/cm $^2$ .

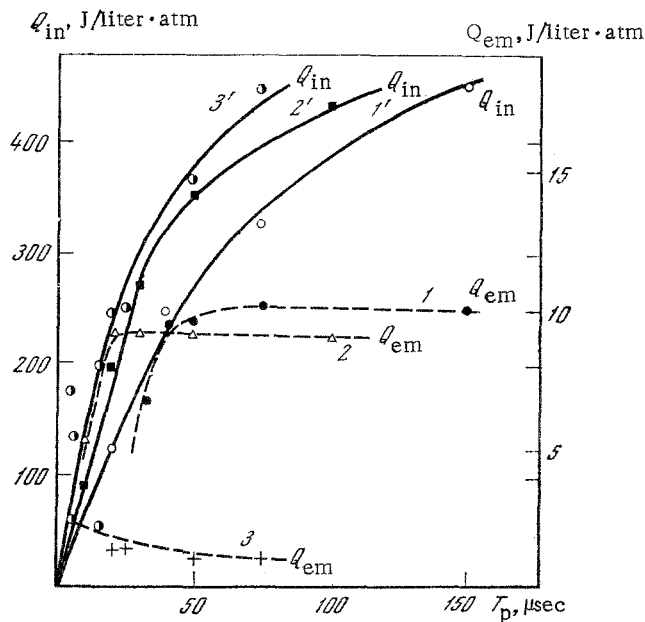


Fig. 9. Dependence of the specific emission energy (1-3) and of the specific energy input (1'-3') on the pump-pulse duration: 1,1') mixture  $\text{CO}_2:\text{N}_2$  (1:2),  $U_0 = 20$  kV,  $T_{\text{out}} = 50\%$ ,  $j_e = 0.7$  mA/cm $^2$ ; 2,2') mixture  $\text{CO}_2:\text{N}_2$  (1:4),  $U_0 = 19$  kV,  $T_{\text{out}} = 50\%$ ,  $j_e = 0.6$  mA/cm $^2$ ; 3,3') mixture  $\text{CO}_2:\text{N}_2$  (1:19),  $U_0 = 18$  kV,  $T_{\text{out}} = 7\%$ ,  $j_e = 0.55$  mA/cm $^2$ .

low ( $\approx 1$  kW/cm $^3$ ) values of the pump power, while the value of  $\tau_{\text{em}}^{\text{max}}$  increases noticeably with increasing  $Q$  of the resonator (inasmuch as the lasing threshold decreases in this case), and the maximum of the  $\tau_{\text{em}}$  ( $W_{\text{pump}}$ ) shifts in this case towards lower excitation intensities. The shortening of the emission pulse with increasing pump power is obviously due to the overheating of the working gas mixture. The slope of the trailing edge of the emission pulse increases with increasing pump power, and the rate of decrease of the value of  $\tau_{\text{em}}$  with increasing  $W_{\text{pump}}$  is larger the smaller the heat capacity of the employed mixture.

The dependence of the lasing efficiency on the pump power, measured in the quasistationary lasing regime ( $T_p = 200$   $\mu$ sec) also has a clearly pronounced maximum that shifts toward higher

values of  $W_{\text{pump}}$  with increasing transparency of the output mirror (Fig. 7). In the regime of "long" pump pulses, the total efficiency, defined as  $Q_{\text{em}}/Q_{\text{pump}}$ , decreases with increasing  $W_{\text{pump}}$  much more rapidly than the effective efficiency shown in Fig. 7, defined as  $Q_{\text{em}}/(\tau_{\text{del}} + \tau_{\text{em}}) \cdot W_{\text{pump}}$ , inasmuch as under intense pumping the lasing stops long before the end of the excitation pulse (Fig. 5).

The best from the point of view of reaching high efficiencies and long lasing duration turned out to be mixtures containing  $\text{CO}_2$  and  $\text{N}_2$  in ratios 1:2-1:4. Addition of helium amounting to  $\sim 50\%$  of the total mixture pressure, at unchanged current density in the electron beam, led to an increase of  $\tau_{\text{em}}$  and  $Q_{\text{em}}$ , but the efficiency decreased, since the energy input increased strongly. Further increase of the nitrogen content in the  $\text{CO}_2:\text{N}_2$  mixture led to a substantial deterioration of the output characteristics. For example, for the mixtures  $\text{CO}_2:\text{N}_2$  (1:9) and (1:19) the total efficiency in all the investigated pump regimes did not exceed several percent.

The decrease of the efficiency with increasing pump power is most probably due to the increase of the gas temperature averaged over the lasing-pulse time. It is known that the efficiency of a  $\text{CO}_2$  laser drops sharply when the gas temperature rises to  $400\text{--}450^\circ\text{K}$ , inasmuch as in this case the rate of depopulation of the upper laser level increases by 2-3 times [21], the cross section for stimulated emission decreases to almost one-half [22], and the population of the lower laser level increases by  $\approx 10$  times. Inasmuch as in the case of strong pumping the temperature of the working gas at which the lasing stops increases almost in proportion to  $W_{\text{pump}}$  [5, 13], and the time during which the gas is heated by  $100\text{--}150^\circ\text{K}$  decreases rapidly with increasing pump, it is clear that the more intense the excitation of the active medium, the larger the fraction of the emission-pulse total duration during which the pumping is certainly ineffective, and consequently the lower should the efficiency be.

In fact, the shortening of the pump pulse duration at a fixed excitation power leads to a noticeable growth of the efficiency (Fig. 8), and at a sufficiently low value of  $T_p$  the total efficiency (i.e.,  $Q_{\text{em}}/Q_{\text{in}}$ ) turns out to be almost equal to the lasing efficiency  $Q_{\text{em}}/Q_{\text{pump}} (\tau_{\text{em}})$ . The decrease of the effective efficiency during the lasing pulse in the case of strong pumping causes the emission energy to cease to increase with increasing excitation-pulse duration, starting with a value of  $T_p$  that depends on the value of  $W_{\text{pump}}$  (Fig. 9).

The increase of the pump power at a fixed ionization-pulse duration and at a constant value of the reduced field intensity in the active region leads to an increase of the emission energy, although the duration of the emission pulse and the efficiency decrease in this case (Fig. 10).

The maximum specific energy output under conditions of quasistationary excitation was  $\sim 30$  J/liter $\cdot$ atm and was obtained with the mixture  $\text{CO}_2:\text{N}_2:\text{He}$  (1:4:5) using an output mirror with transparency 50%. In a resonator with high  $Q$ , when the specific energy output was increased to  $\sim 10$  J/liter $\cdot$ atm, the output mirror was damaged.

#### I.4. Discussion of Results. Choice of Optimal Conditions of Excitation of EB Laser

Other results obtained in the experiments agree qualitatively well with the results of a numerical calculation of the characteristics of a  $\text{CO}_2$ -EBL operating in the continuous excitation regime [13]. No quantitative agreement was reached with the theoretical data of [13], and the efficiency and particularly the lasing-pulse duration turned out to be much lower than expected. In our opinion, the reason is that the calculations were performed under idealized conditions it was assumed that the reduced field intensity is

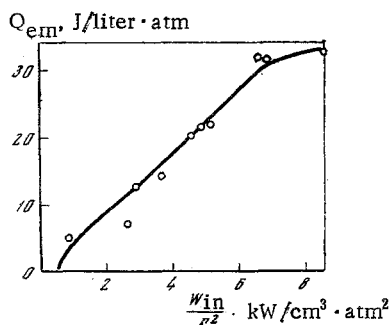


Fig. 10. Dependence of the specific energy output on the average reduced pump power. Mixture  $\text{CO}_2:\text{N}_2:\text{He}$  (1:4:5),  $p = 0.5$  atm,  $T_{\text{out}} = 50\%$ ,  $T_p = 100$   $\mu\text{sec}$ ,  $E/p = 3$  kV/cm $\cdot$ atm.

TABLE 1

T, K	$\sigma$ , cm <sup>-2</sup>	$\alpha_{\text{thr}}/\sigma$ , cm <sup>-3</sup>	$N_{\text{CO}_2} \times \exp(-h\nu/kT_f)$	$\tau$ , $\mu\text{sec}$	$W_{\text{thr}}$ , W/cm <sup>3</sup>
300	$1.5 \cdot 10^{-18}$	$3 \cdot 10^{15}$	$2.7 \cdot 10^{15}$	5,5	61
400	$1 \cdot 10^{-18}$	$4.5 \cdot 10^{15}$	$1.5 \cdot 10^{16}$	3,9	290
500	$7.2 \cdot 10^{-19}$	$6.1 \cdot 10^{15}$	$4.2 \cdot 10^{16}$	2,6	1100
600	$5.5 \cdot 10^{-19}$	$8.2 \cdot 10^{15}$	$8.3 \cdot 10^{16}$	1,7	3200

optimal, that the working gases contain no impurities whatever, that the mirrors do not absorb and do not scatter the radiation, and that the pumping is perfectly uniform over the entire volume of the active region. These conditions were certainly not satisfied in the experiment, inasmuch as, first, we used N<sub>2</sub> and CO<sub>2</sub> of technical purity, second, operation at optimal E/p turned out to be practically impossible because of development of breakdown in the gas. As a result of reflection of the fast electrons from the anode and of the weakening of the field on the periphery of the discharge, the distribution of the pump power over the cross section of the discharge gap was not uniform. For a direct comparison of the experimental data with the theoretical ones it is therefore necessary to carry out numerical simulation of the laser with account taken of the actual experimental conditions.

For a qualitative analysis of the operation of a CO<sub>2</sub>-EBL under continuous and quasi-continuous excitation, we shall derive several simple relations. The output laser energy emitted during the lasing time can be expressed as  $Q_{\text{em}} = W_{\text{pump}} \cdot \tau_{\text{em}} \cdot \eta$ . Lasing begins after the threshold inversion value is reached:

$$\Delta N_{\text{thr}} \simeq (N_{00^1})_{\text{thr}} = \frac{\alpha_{\text{thr}}}{s(T_0)} = \frac{1}{2Ls} \ln \frac{1}{R_1 R_2} \quad (2)$$

and is extinguished as a result of the increase of the effective lasing threshold with increasing temperature, due to the thermal population of the lower laser level (1), to the decrease of the lifetime of the upper laser level  $\tau$  (2), and to the decrease of the cross section  $\sigma$  of the stimulated emission (3):

$$(N_{00^1} - N_{100})_{\text{thr, fin}} \simeq \frac{W_{\text{pump}}}{h\nu_{00^1}} \gamma_{12} \tau(T_f) - \beta N_{\text{CO}_2} \exp(-h\nu_{10^0}/kT_f) = \frac{\sigma_{\text{thr}}}{\sigma(T_f)}. \quad (3)$$

Here  $N_{\text{CO}_2}$  is the density of the CO<sub>2</sub> molecules in the working mixture;  $\beta \leq 1$ , a coefficient that takes into account the redistribution of the CO<sub>2</sub> molecules among the levels 10°0 and 02°0;  $T_0$ , initial gas temperature;  $T_f$ , final gas temperature at which the lasing stops. The gas temperature is determined by its heat capacity  $C_g$  and by the pump energy converted into heat:

$$\Delta T_g = \frac{W_{\text{pump}} \tau_{\text{pump}} (1 - \eta)}{C_g}. \quad (4)$$

The quantities  $N_{10^0}$ ,  $\sigma$  and  $\tau$ , calculated for several values of the gas temperature, are given in Table 1. The calculations were performed for the mixture CO<sub>2</sub>:N<sub>2</sub>:He (1:4:5) at a pressure 1 atm, and the value of  $\tau(300^\circ\text{K})$  was determined from the lasing threshold in the present study. The temperature dependences of  $\sigma$  and  $\tau$  were calculated in accordance with the data of [22-25] and [21]. It was assumed that  $\alpha_{\text{thr}} \simeq 4.5 \cdot 10^{-3}$  cm<sup>-1</sup> (this corresponds to a mirror reflection coefficient 100% and 40% at an active-region length 100 cm), and  $\gamma_{1,2} \simeq 0.8$  [17].

Although the data of Table 1 are only estimates, they make it possible to compare the qualitative picture of the variation of the lasing duration as a function of the pump power. It is clear that at low excitation levels the lasing is stopped in the main ( $W_{\text{pump}} \geq W_{\text{thr}}$ ) because of the deterioration of the resonator Q and of the decreased efficiency of the pumping, both of which are determined by the decrease of the values of  $\sigma$  and  $\tau$ , respectively, and the increase of  $N_{100}$  can be neglected in this case.

According to (3), the final gas temperature then increases almost linearly with the pump:



$$T_f \simeq \left[ \frac{W_{\text{pump}}}{h\nu_{001}} \gamma_{12} \tau (300^\circ) + \alpha_{\text{thr}} \cdot 3,8 \cdot 10^{15} \cdot 130 \right] / \left[ \frac{W_{\text{pump}}}{h\nu_{001}} \gamma_{12} \tau (300^\circ) \cdot 1,4 \cdot 10^{-3} + \alpha_{\text{thr}} \cdot 3 \cdot 8 \cdot 10^{15} \right]. \quad (5)$$

The numerical coefficients are determined here by approximating the functions  $\sigma^{-1}(T) \approx 3,8 \cdot 10^{15} (T - 130^\circ) \text{ cm}^2$  [22],  $\tau(T) \approx 5,5 \cdot 10^{-6} (1 - 1,4 \cdot 10^{-3} T) \text{ sec}$  [21]. Accordingly, at high pump powers the interruption of the lasing is determined by the thermal population of the lower level. In this case

$$T_f \simeq h\nu_{100} \left[ k \ln \left( \frac{h\nu_{001} \beta N_{\text{CO}_2}}{W_{\text{pump}} \gamma_{12} \tau_0} \right) \right] \quad (6)$$

and the limiting temperature increases logarithmically with the pump. It is easily seen that in this case the lasing duration first increases:

$$\tau_{\text{em}} \simeq \frac{C_g}{1-\eta} \left[ \left( \frac{\gamma_{12} \tau_0}{h\nu_{001}} + \frac{\alpha_{\text{thr}}}{W_{\text{pump}}} \cdot 5 \cdot 10^{17} \right) / \left( W_{\text{pump}} \frac{\gamma_{12} \tau_0}{h\nu_{001}} 1,4 \cdot 10^{-3} + \alpha_{\text{thr}} \cdot 3 \cdot 10^{15} \right) \right], \quad (7)$$

since the efficiency in this regime increases practically linearly with the pump power:

$$\eta \simeq \frac{h\nu_{\text{em}}}{h\nu_{001}} \gamma_{12} \left( 1 - \frac{W_{\text{thr}}}{W_{\text{pump}}} \right), \quad (8)$$

and in the case of intense pumping  $\tau_{\text{em}}$  decreases monotonically:

$$\tau_{\text{em}} \simeq \frac{C_r}{1-\eta} \frac{h\nu_{100}}{k} \left[ W_{\text{pump}} \ln \left( \frac{h\nu_{001} \beta N_{\text{CO}_2}}{W_{\text{pump}} \gamma_{12} \tau_0} \right) \right]^{-1}. \quad (9)$$

In analogy with relations (7) and (9), we can obtain from (8), with the aid of (3) and (4), the dependence of the efficiency on the excitation time for the cases of weak and strong pumping.

The obtained approximate  $T_f(W_{\text{pump}})$ ,  $\tau_{\text{em}}(W_{\text{pump}})\eta(T_p)$ , and  $\eta(W_{\text{pump}})$  dependences are in qualitatively good agreement with the results of numerical calculations [13]. It is clear that for other  $\text{CO}_2:\text{N}_2:\text{He}$  mixtures one obtains similar relations with different numerical coefficients.

Although the relations obtained are rather cumbersome, they do permit a number of conclusions to be drawn with respect to the choice of the optimal excitation regime of an EB laser. The average emission power in the repeated-pulse regime with a pulse-repetition frequency  $f$  will obviously be  $\bar{W}_{\text{em}} \approx fQ_{\text{em}}$  ( $Q_{\text{em}}$  is the energy of an individual emission pulse). Since the limiting repetition frequency at a flow velocity  $v$  amounts to  $f \approx v/a$ , where  $a$  is the transverse dimension of the active region in the flow direction and  $T_p \ll 1/f$ , the maximum average emission power in this regime can be expressed as follows:

$$(\bar{W}_{\text{em}})_{\text{max}} \simeq \frac{v}{a} \frac{\eta}{1-\eta} C_g h\nu_{100} \left[ k \ln \left( \frac{h\nu_{001} \beta N_{\text{CO}_2}}{W_{\text{pump}} \gamma_{12} \tau_0} \right) \right]^{-1}. \quad (10)$$

We consider the case  $W_{\text{pump}} \gg W_{\text{thr}}$ , since at  $W_{\text{pump}} \approx W_{\text{thr}}$  the energy output in each individual pulse is too small. From (8) we easily obtain

$$\frac{\eta}{1-\eta} \simeq \gamma_{\text{qu}} \gamma_{12} \left( 1 - \gamma_{\text{qu}} \gamma_{12} + \frac{W_{\text{thr}}}{W_{\text{pump}}} \right)^{-1}. \quad (11)$$

It follows from (10) and (11) that to obtain the maximum average emission energy in this case it is necessary to ensure the highest possible efficiency in each individual lasing pulse, and this high efficiency must be reached at a high pump power by lowering of the effective lasing threshold. Consequently, the optimal pumping is produced by powerful pulses that are so short that  $\tau_{\text{em}} > \tau_{\text{pump}}$ . It was in precisely this regime that the maximum specific energy

outputs were obtained in experiments from an EB CO<sub>2</sub> laser [4, 11]. The limit of the pump power is determined in this case, first, by the breakdown of the gas as a result of the overheat instabilities that develop at  $W_{\text{pump}} \gtrsim 40\text{--}50 \text{ kW/cm}^3$  [4]; second, by the breakdown strength of the mirrors (experiments [15] have shown, e.g., that the best single-layer dielectric mirrors on NaCl substrates and having  $R_{\text{ref}} = 30\text{--}40\%$  can withstand fluxes up to  $10\text{--}12 \text{ J/cm}^2$  at emission-pulse durations  $10\text{--}20 \text{ } \mu\text{sec}$ ); third, by the breakdown strength of the working gas medium, which according to the data of [26] amounts to  $10^9 \text{ J/cm}^2$  for emission pulses of duration  $\gtrsim 10^{-6} \text{ sec}$ . It must be emphasized that the use of short ( $T_p < \tau_{\text{em}}$ ) active-medium ionization pulses makes it possible to use effectively also the energy introduced into the active medium on the recombination "tail" of the discharge-current pulse. One other advantage of short  $\lesssim 10\text{--}20 \text{ } \mu\text{sec}$  excitation pulses is the small change of the stimulated-emission cross section even at very high pump levels, inasmuch as the increase of the gain line width with increasing temperature is determined only by the temperature dependence of the gas density [21], and the gas density hardly manages to change within a time  $\sim 10 \text{ } \mu\text{sec}$ .

As shown by the experiments reported in this paper as well as by the investigations of the operation of CO<sub>2</sub>-EBL at maximum excitation pulses, which were performed by us earlier [4, 5], the gas mixture that is optimal from the point of view of obtaining maximum efficiency in an individual lasing pulse of duration  $10\text{--}30 \text{ } \mu\text{sec}$  using reasonable field intensities in the discharge gap ( $\sim 4 \text{ kV/cm}\cdot\text{atm}$ ) is a mixture containing CO<sub>2</sub> and N<sub>2</sub> in a ratio (1:2)-(1:4) and 30-50% He (these data pertain to mixtures of commercial gases). The pump power is determined in practice by the current density in the fast-electron beam of the employed electron gun. Let us estimate by way of example the possible characteristics of a repeated-pulse laser using the mixture CO<sub>2</sub>:N<sub>2</sub>:He (1:4:5) at  $p = 1 \text{ atm}$  and  $j_e \approx 1 \text{ mA/cm}^2$ . In accord with the experimental results, we put  $b \approx 1.3 \cdot 10^{-7} \text{ cm}^3/\text{sec}$ ,  $\mu = 1.25 \cdot 10^3 \text{ cm}^2/\text{V}\cdot\text{sec}$ , and  $n_e = 3.4 \cdot 10^{12} \text{ cm}^{-3}$ . At  $E/p = 4 \text{ kV/cm}\cdot\text{atm}$  the pump power is  $W_{\text{pump}} \approx 10.8 \text{ kW/cm}^3$ . The emission duration for this pump is  $\sim 30 \text{ } \mu\text{sec}$  and is practically independent of the resonator Q, see Eq. (9). Choosing  $T_p = 15 \text{ } \mu\text{sec}$ , we obtain  $Q_{\text{in}} \approx 200 \text{ J/liter}$  (with account taken of the recombination "tail" of the current pulse) and  $\eta \approx 20\%$ , so that  $Q_{\text{em}} \approx 40 \text{ J/liter}$ . At a gas flow velocity  $v = 100 \text{ m/sec}$  and  $a = 20 \text{ cm}$  we have  $f_{\text{max}} = 500 \text{ pulses/sec}$ , and accordingly  $(\bar{W}_{\text{em}})_{\text{max}} \approx 20 \text{ kW/liter}$ . To ensure a small beam divergence, the pulse repetition frequency must usually be decreased by a factor 2-3 compared with  $f_{\text{max}}$ , so that in the considered example  $(\bar{W}_{\text{em}})_{\text{max}}$  should amount to  $\sim 10 \text{ kW/liter}$ . To increase the average power it is necessary to increase the flow rate and the current density in the electron beam. We note that an increase of the pump-pulse duration to  $\sim 50 \text{ } \mu\text{sec}$  at the same power was shown by experiment to lead not to an increase of  $Q_{\text{em}}$ , but to a sharp decrease of the lasing efficiency in each individual pulse — to a value of the order of 3-5%. An increase of the pump pulse duration to  $T_p \approx 100 \text{ } \mu\text{sec}$  with a simultaneous lowering of the pump power to a level such that  $\tau_{\text{em}} \gtrsim T_p$  leads to a decrease of the energy output, for even in a resonator with relatively high Q (e.g., at  $R_{\text{ref}} \approx 50\%$  and  $L = 200 \text{ cm}$ ) numerical calculation [13] shows that to obtain  $\tau_{\text{em}} \approx 100 \text{ } \mu\text{sec}$  for 1:4:5 mixture it is necessary to decrease the pump power to  $W_{\text{pump}} \approx 900 \text{ W/cm}^3$  (in this case  $\eta \approx 18\%$ ). It is easily seen that in such a regime  $Q_{\text{em}} \approx 16 \text{ J/liter}$ . In fact, the pump level at which  $\tau_{\text{em}} = 100 \text{ } \mu\text{sec}$ , as shown by experiments, is even lower and consequently  $Q_{\text{em}}$  is still lower.

## II. EXPERIMENTAL INVESTIGATION OF THE INFLUENCE OF ADDITION OF HYDROGEN ON THE ENERGY CHARACTERISTICS OF AN ELECTRON-BEAM-CONTROLLED LASER

Electrically excited CO<sub>2</sub> lasers usually employ CO<sub>2</sub>:N<sub>2</sub>:He mixtures. This composition is used both in the pulsed and the cw regimes. The role of each component of this mixture is well known: CO<sub>2</sub> is the active medium. N<sub>2</sub> is the reservoir of the vibrational energy stored here in the course of pumping and transferred to the upper laser level as a result of a resonant v-v process; the helium is needed, first, to increase the electron temperature of the discharge and, second, to increase the rate of depopulation of the lower laser level. In addition, in open-cycle-flow CO<sub>2</sub> lasers of low pressure, an important role of helium is the improvement of the heat dissipation from the active region [27, 28]. The optimum content of each of these components is determined by the operating regime of the CO<sub>2</sub> laser. As a rule, the fraction of the helium in cw low-pressure lasers excited by a longitudinal self-sustaining discharge is 70-90% [27-29], and 30-50% in high-power pulsed electron-beam-controlled lasers [12]. The highest values of the specific emission energy and efficiency of pulsed EB CO<sub>2</sub> atmospheric-pressure lasers were obtained using the CO<sub>2</sub>:N<sub>2</sub>:He mixtures with ratios (1:1:2)-(1:2:3) [12], while for cw EB CO<sub>2</sub> lasers the optimum mixture turned out to be CO<sub>2</sub>:N<sub>2</sub>:He (1:30:16) [30]. At the same time, in connection with research

TABLE 2

Installation parameters	First installation ("short" pulse regime)	Second installation ("long" pulse regime)
Dimensions of active region, cm	2,5×4×100	7×7,5×100
Duration of ionization pulse, μsec	0,6	20-100
Fast-electron energy, keV	160	100
Current density in the electron beam entering the discharge gap, mA/cm	400	1-15
Operating range of fields in the discharge gap, kV/cm · atm	2-7	2-5
Specific pump power, kW/cm <sup>3</sup>	up to 100	up to 10

into various applications of EB CO<sub>2</sub> lasers and the production of installations with large active volumes and correspondingly large gas-mixture consumption, it becomes urgent to find a working mixture having sufficiently high lasing characteristics but not containing the expensive helium. It is easy to show, e.g., that for a 20-kW EB CO<sub>2</sub> laser using a mixture containing 50% He, with a specific energy output 50 J/g in the mixture-recirculation regime with replenishment of 0.5% of the gas after each circulation cycle, the helium consumption amounts to ~3.5 m<sup>3</sup>/h.

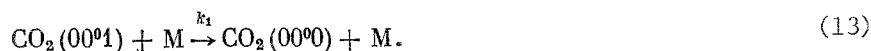
Inasmuch as in electron-beam-controlled excitation it is possible to optimize the electron temperature of the discharge in a mixture containing CO<sub>2</sub> even in the absence of He, the only fundamental reason for introducing helium into the working mixture of the EB CO<sub>2</sub> laser is the need for increasing the rate of depopulation of the lower laser level. It is known that, besides He, a high rate of depletion of the 01<sup>1</sup>0 CO<sub>2</sub> level, which determines the rate of depopulation of the lower laser level (10<sup>0</sup>0, 02<sup>2</sup>0), can be produced also by molecules such as H<sub>2</sub>O, H<sub>2</sub> and D<sub>2</sub>. The rate constants of the process



for these molecules are [31-33]

$$k, \text{ torr}^{-1} \cdot \text{sec}^{-1} \quad \begin{array}{c} \text{M} \\ \text{He} \quad \text{H}_2\text{O} \quad \text{H}_2 \quad \text{D}_2 \\ 3.8 \cdot 10^3 \quad 5 \cdot 10^3 \quad 8 \cdot 10^4 \quad 2 \cdot 10^4 \end{array}$$

but, in contrast to He, all these molecules depopulate also the upper laser level:



This process is characterized by the following constants [31, 33]:

$$k_1, \text{ torr}^{-1} \cdot \text{sec}^{-1} \quad \begin{array}{c} \text{M} \\ \text{He} \quad \text{H}_2\text{O} \quad \text{H}_2 \quad \text{D}_2 \\ 68 \quad 4 \cdot 10^4 \quad 5 \cdot 10^3 \quad 270 \end{array}$$

We have experimentally investigated in the present study the possibility of replacing the helium by hydrogen in the working gas mixtures of an atmospheric-pressure EB CO<sub>2</sub> laser. The possibility of using deuterium and water vapor for this purpose was not analyzed by us, since deuterium is even more expensive than helium, and the optimum concentration of the water vapor at a pump-pulse duration  $\geq 0.1$  μsec cannot exceed 0.01-0.1%, owing to the higher rate of depopulation of the upper laser level by the H<sub>2</sub>O molecules. Exact control of a water-vapor pressure on the order of 0.1-0.5 torr in a mixture of atmospheric pressure is a rather complicated technical task, and an increase of the H<sub>2</sub>O pressure to 1-2 torr, as shown by our experience, exerts a substantially adverse effect on both the dielectric strength of the CO<sub>2</sub>:N<sub>2</sub> mixture and on its lasing characteristics. The use of hydrogen is therefore preferable for technical installations.

The impact of hydrogen on the operation of an EB CO<sub>2</sub> laser was the subject of [34-36]. It was observed in [34] that addition of H<sub>2</sub> affects favorably the characteristics of an EB amplifier using a CO<sub>2</sub>:N<sub>2</sub> mixture and excited by short ( $\sim 10^{-7}$  sec) pulses. It was noted in [35] that at low ( $\sim 210^\circ\text{K}$ ) temperature of the active medium the use of the mixture CO<sub>2</sub>:N<sub>2</sub>:H<sub>2</sub>

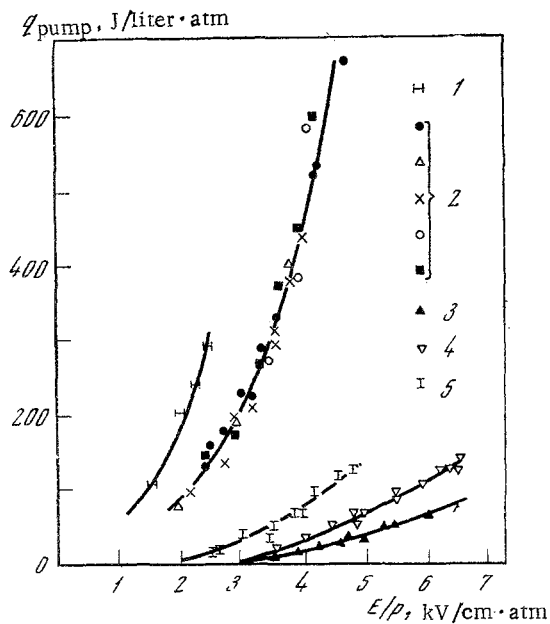


Fig. 11. Dependence of the specific pump energy  $q_{\text{pump}}$  on the reduced field intensity in the discharge gap:  $\text{CO}_2:\text{N}_2:\text{He}$ : 1) (1:2:0:3); 2) (1:2:0:0), (1:2:0.5:0), (1:2:0.25:0), (1:2:0.125:0), (1:2:0.062:0); 3) (1:1:0:0); 4) (1:1:1:0); 5) (1:1:0:3); 1, 2)  $p = 0.5$  atm,  $\tau_{\text{pump}} = 70$   $\mu\text{sec}$ ;  $j_e = 15$   $\text{mA}/\text{cm}^2$ ; 3-5)  $p = 1$  atm,  $\tau_{\text{pump}} = 1$   $\mu\text{sec}$ ;  $j_e \approx 0.4$   $\text{A}/\text{cm}^2$ .

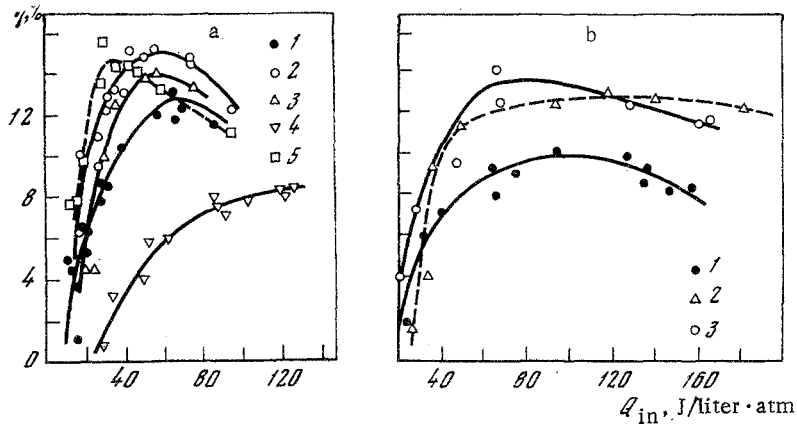


Fig. 12. Dependence of the efficiency of an EB  $\text{CO}_2$  laser on the specific pump energy at  $\tau_{\text{pump}} = 1$   $\mu\text{sec}$  and  $p = 1$  atm: a)  $\text{CO}_2:\text{N}_2:\text{H}_2:\text{He}$  [1) (1:1:0:0), 2) (1:1:0.17:0), 3) (1:1:0.08:0), 4) (1:1:1:0), 5) (1:1:0:3)]; b)  $\text{CO}_2:\text{N}_2:\text{H}_2:\text{He}$  [1) (1:4:0:0), 2) (1:4:0.5:0), 3) (1:4:0:5)].

(1:3:0.08) in a pulsed ( $\tau_{\text{pump}} = 25$   $\mu\text{sec}$ ) laser yields the same specific energy output and efficiency as a  $\text{CO}_2:\text{N}_2:\text{He}$  (1:2:3) mixture at the same pressure. The authors of [36] have reached, as a result of numerical calculations, the conclusion that addition of hydrogen should increase the efficiency of pulsed EB  $\text{CO}_2$  lasers at all pump powers. So far, however, no detailed investigations were made of EB lasers with  $\text{CO}_2:\text{N}_2:\text{H}_2$  mixture, nor were the lasing characteristics of mixtures with helium and hydrogen compared and the compositions of hydrogen-containing mixtures for various excitation regimes optimized.

The experiments in the present study were performed with two setups in two typical pumping regimes. The parameters of the setups are listed in Table 2.

For convenience in the comparison of the results, the two installations had identical hemispherical resonators, consisting of a concave copper mirror (curvature radius 5 m) and a plane-parallel germanium plate.

We have investigated the energy and temporal characteristics of the laser emission, as well as the parameters of the non-self-sustaining discharge at various hydrogen concentrations in the  $\text{CO}_2:\text{N}_2:\text{H}_2$  mixtures. Measurements under the same conditions were performed also for the corresponding  $\text{CO}_2:\text{N}_2:\text{He}$  mixtures containing  $\sim 50\%$  He.

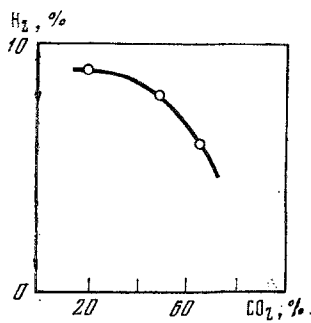


Fig. 13

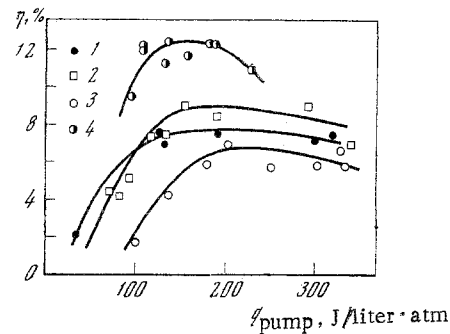


Fig. 14

Fig. 13. Dependence of the optimal hydrogen content in the CO<sub>2</sub>:N<sub>2</sub>:H<sub>2</sub> mixture on the CO<sub>2</sub> content in the initial CO<sub>2</sub>:N<sub>2</sub> mixture ( $p = 1$  atm,  $\tau_{\text{pump}} = 1$   $\mu\text{sec}$ ,  $j_e = 0.4$  A/cm<sup>2</sup>).

Fig. 14. Dependence of the efficiency of the EB CO<sub>2</sub> laser on the specific pump energy in the "long" pulse regime ( $\tau_{\text{pump}} = 20$   $\mu\text{sec}$ ,  $j_e = 15$  mA/cm<sup>2</sup>,  $p = 0.5$  atm): CO<sub>2</sub>:N<sub>2</sub>:H<sub>2</sub>:He [1] (1:2:0:0), 2) (1:2:0.06:0), 3) (1:2:0.5:0), 4) (1:2:0:3)].

Typical dependences of the specific energy input on the reduced field intensity in the discharge gap are shown in Fig. 11. It turned out that in both excitation regimes the specific energy input and the breakdown field intensity (at which streamer breakdown develops in the discharge gap following a non-self-sustaining discharge pulse) are practically independent of the hydrogen concentration in the CO<sub>2</sub>:N<sub>2</sub>:H<sub>2</sub> mixture. Only when the H<sub>2</sub> content is increased to ~30% did we observe in the "short" pulse regime a certain increase of the specific energy input, due apparently to the decrease of the coefficient of electron-ion recombination and to the increase of the drift velocity in the CO<sub>2</sub>:N<sub>2</sub>:H<sub>2</sub> mixture compared with the CO<sub>2</sub>:N<sub>2</sub> mixture [14]. At identical values of the parameter  $E/p$ , the input into the CO<sub>2</sub>:N<sub>2</sub>:He mixture is much higher than into a CO<sub>2</sub>:N<sub>2</sub>:H<sub>2</sub> having the same CO<sub>2</sub> and N<sub>2</sub> concentration ratio, but owing to the lower dielectric strength of the mixtures with helium, the maximum energy input  $q_{\text{pump}}^{\text{max}}$  for them turned out to be much lower. This difference manifests itself stronger the longer the pump pulse and the more nitrogen in the mixture. Figure 12 shows typical plots of the laser efficiency vs the specific energy input, measured in the short-pulse regime. With increasing H<sub>2</sub> concentration, the maximum efficiency first increases, shifting towards lower energy inputs, and reaches practically the same value for the mixture with optimum H<sub>2</sub> content as for the mixture with helium, after which it decreases, shifting again towards the higher energy inputs. Similar dependences were observed in the short-pulse regime for all the investigated CO<sub>2</sub>:N<sub>2</sub> mixtures, and only the optimal hydrogen content with respect to efficiency changed (Fig. 13). In the "long" pulse regime (see Fig. 14) the efficiency also first increases with increasing hydrogen content, after which it begins to decrease, but the maximum efficiency for CO<sub>2</sub>:N<sub>2</sub>:H<sub>2</sub> mixtures in this regime turned out to be somewhat lower than for the corresponding CO<sub>2</sub>:N<sub>2</sub>:He mixtures. The optimum H<sub>2</sub> content in this regime is 1-3%. The relation between the values of the maximum emission energies  $q_{\text{em}}^{\text{max}}$  for mixtures with helium and hydrogen, as can be easily seen, depends on the excitation regime. In the regime where short powerful pump pulses are used, the maximum values of the efficiency are approximately equal, but owing to the higher dielectric strength of the helium-free mixtures, and the correspondingly larger values of the maximum energy input, the use of CO<sub>2</sub>:N<sub>2</sub>:H<sub>2</sub> mixtures can result in higher emission energies. In the long-pulse regime, the decrease of the efficiency and increase of the limiting energy input when helium is replaced by hydrogen cancel each other. To illustrate these conclusions, Tables 3 and 4 give the limiting (under the experimental conditions) energy characteristics of certain CO<sub>2</sub>:N<sub>2</sub>:H<sub>2</sub> and CO<sub>2</sub>:N<sub>2</sub>:He mixtures.

Figure 15 shows plots of the lasing delay times  $\tau_{\text{del}}$  and of the emission-pulse duration  $\tau_{\text{em}}$  versus the specific pump power  $W_{\text{pump}}$ . At low pump intensity ( $j_e \approx 1$  mA/cm<sup>2</sup>) the lasing delay increases monotonically, and the duration of the emission pulse decreases with increasing H<sub>2</sub> content, but the general character of the  $\tau_{\text{del}}(W_{\text{pump}})$  and  $\tau_{\text{em}}(W_{\text{pump}})$  plots and of their ratio remains unchanged. The value of  $\tau_{\text{del}}$  for the CO<sub>2</sub>:N<sub>2</sub> mixture turns out to be lower under these conditions, for all values of the parameter  $E/p$ , than for mixtures with hydrogen (the corresponding curve practically coincides with curve 3 of Fig. 15a). At high pump power and

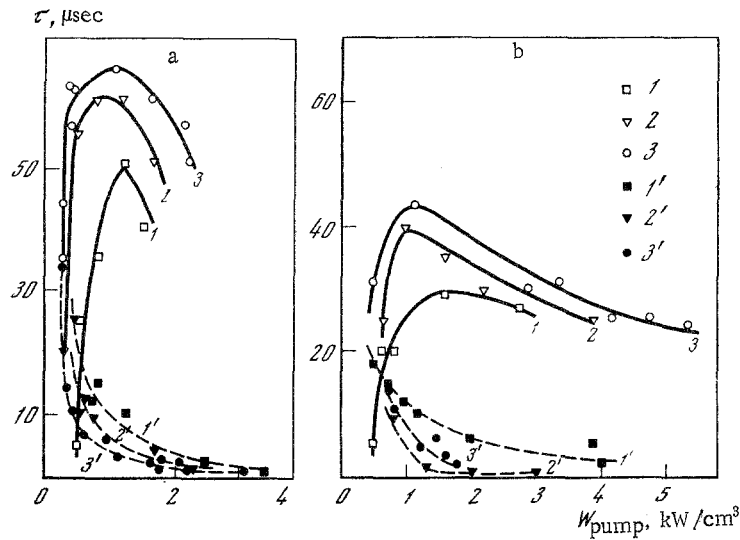


Fig. 15. Dependences of the radiation pulse (1-3) and of the lasing delay pulse (1'-3') on the specific pump power,  $p = 0.5$  atm,  $\tau_{\text{pump}} \approx 70$   $\mu\text{sec}$ ,  $\text{CO}_2:\text{N}_2:\text{H}_2$ : 1) (1:2:0.25); 2) (1:2:0.125); 3) (1:2:0.06); a)  $j_e = 1$   $\text{mA}/\text{cm}^2$ ; b)  $j_e = 15$   $\text{mA}/\text{cm}^2$ .

TABLE 3

Composition of working mixture	$q_{\text{pump}}^{\text{max}}$ , J/liter·atm	$q_{\text{em}}^{\text{max}}$ , J/liter·atm	Eff., %	Composition of working mixture	$q_{\text{pump}}^{\text{max}}$ , J/liter·atm	$q_{\text{em}}^{\text{max}}$ , J/liter·atm	Eff., %
$\text{CO}_2:\text{N}_2(1:4)$	180	13	10	$\text{CO}_2:\text{N}_2(1:1)$	140	10	13
$\text{CO}_2:\text{N}_2:\text{H}_2(1:4:0,5)$	200	22	12,5	$\text{CO}_2:\text{N}_2:\text{H}_2(1:1:0,17)$	140	12	15
$\text{CO}_2:\text{N}_2:\text{He}(1:4:5)$	170	19	13	$\text{CO}_2:\text{N}_2:\text{He}(1:1:3)$	120	10	15
$\text{CO}_2:\text{N}_2(1:2)$	150	10	8	$\text{CO}_2:\text{N}_2(2:1)$	70	6	11
$\text{CO}_2:\text{N}_2:\text{H}_2(1:2:0,06)$	1600	19	14	$\text{CO}_2:\text{N}_2:\text{H}_2(2:1:0,25)$	85	11	14
$\text{CO}_2:\text{N}_2:\text{He}(1:2:1,5)$	130	13	14,5	$\text{CO}_2:\text{N}_2:\text{He}(2:1:3)$	60	7	16

Note.  $p = 1$  atm,  $\tau_{\text{pump}} = 1$   $\mu\text{sec}$ .

TABLE 4

Composition of working mixture	$\tau_{\text{pump}} = 20$ $\mu\text{sec}$			$\tau_{\text{pump}} = 70$ $\mu\text{sec}$		
	$q_{\text{pump}}^{\text{max}}$ , J/liter·atm	$q_{\text{em}}^{\text{max}}$ , J/liter·atm	Max. eff., %	$q_{\text{pump}}^{\text{max}}$ , J/liter·atm	$q_{\text{em}}^{\text{max}}$ , J/liter·atm	Max. eff., %
$\text{CO}_2:\text{N}_2(1:2)$	320	24	8	600	18	3
$\text{CO}_2:\text{N}_2:\text{H}_2(1:2:0,06)$	350	20	9	600	26	5,1
$\text{CO}_2:\text{N}_2:\text{He}(1:2:3)$	230	23	12	250	25	11
$\text{CO}_2:\text{N}_2(1:4)$	330	25	8	600	21	3,5
$\text{CO}_2:\text{N}_2:\text{H}_2(1:4:0,125)$	340	30	10	610	30	6
$\text{CO}_2:\text{N}_2:\text{He}(1:4:5)$	325	20	12	300	30	10

Note.  $j_e = 10-15$   $\text{mA}/\text{cm}^2$ ,  $p = 0.5$  atm. The efficiency values given for  $\tau_{\text{pump}} = 70$   $\mu\text{sec}$  were calculated relative to the total pump energy (the efficiencies are in this case low, since the lasing stops prior to the end of the pump pulse, owing to the heating of the mixture).

low values of  $E/p$  ( $\leq 2$   $\text{kV}/\text{cm}\cdot\text{atm}$ ) the growth of the delay time with increasing  $\text{H}_2$  concentration ceases to be monotonic, and in this case the mixtures having the minimum delay time are those with increased  $\text{H}_2$  content (see Fig. 15b; the curves of Fig. 15a were plotted at  $E/p$  values from 3 to 6  $\text{kV}/\text{cm}\cdot\text{atm}$ , while those of Fig. 15b were plotted at  $E/p$  from 1 to 4 at  $\text{kV}/\text{cm}\cdot\text{atm}$ ).

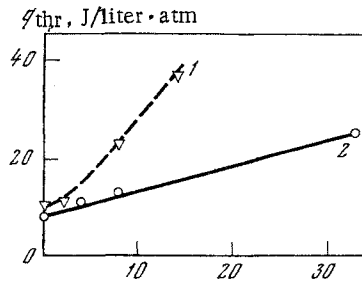


Fig. 16

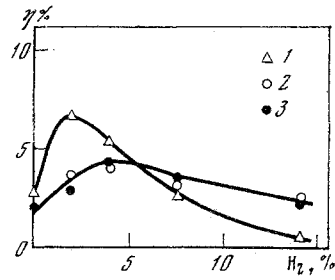


Fig. 17

Fig. 16. Dependence of the threshold pump energy on the hydrogen content in the  $\text{CO}_2:\text{N}_2:\text{H}_2$  mixture for the component ratios: 1)  $\text{CO}_2:\text{N}_2$  (1:2),  $p = 0.5$  atm,  $E/p = 2.5$  kV/cm·atm,  $W_{\text{pump}} = 300\text{--}500$  W/cm<sup>3</sup>; 2)  $\text{CO}_2:\text{N}_2$  (1:1),  $p = 1$  atm,  $E/p = 3.5$  kV/cm·atm,  $W_{\text{pump}} = 10\text{--}20$  W/cm<sup>3</sup>.

Fig. 17. Dependence of the efficiency on the hydrogen content in the mixture  $\text{CO}_2:\text{N}_2:\text{H}_2$  ( $\text{CO}_2:\text{N}_2$  (1:2),  $p = 0.5$  atm,  $E/p = 4$  kV/cm·atm,  $\tau_{\text{pump}} = 60$   $\mu\text{sec}$ ): 1)  $j_e = 1$  mA/cm<sup>2</sup>, 2)  $j_e = 10$  mA/cm<sup>2</sup>, 3)  $j_e = 15$  mA/cm<sup>2</sup>.

The analysis of the results becomes particularly lucid when simple expressions are used for the delay time and for the efficiency of the  $\text{CO}_2$  laser. These expressions can be easily obtained in the two-level approximation for a quasistationary lasing regime, neglecting the gas heating [15, 12]:

$$\tau_{\text{del}} \approx \tau_{00^1} \frac{1+\delta}{\delta} \ln \left[ 1 - \frac{h\nu_{00^1}}{\gamma W_{\text{pump}} \tau_{00^1}} \left( \frac{\alpha_{\text{thr}}}{\sigma} + N_{10^0} \right) \right]^{-1}; \quad (14)$$

$$\eta \approx \frac{\nu_{em}}{\nu_{00^1}} \gamma \frac{1-R}{\ln(1/R)} \left( 1 - \frac{q_{\text{thr}}}{q_{\text{pump}}} \right) \left[ \left( 1 - \frac{\gamma_{00^1} \gamma_{10^0} \tau_{10^0}}{\gamma_{10^0} \gamma \tau_{00^1}} - \frac{\text{thr} \tau_{\text{pump}}}{\sigma \tau_{00^1}} \frac{h\nu_{00^1}}{\gamma q_{\text{pump}}} \right) \left( 1 + \frac{\tau_{10^0}}{\tau_{00^1}} \right) \right], \quad (15)$$

$$N_{10^0} \approx N_0 \left[ \exp \left( -\frac{h\nu_{01^0}}{kT_g} \right) + \frac{(1-\gamma) W_{\text{pump}} \tau_{01^0}}{N_0 h\nu_{01^0}} \right]^2; \quad (16)$$

$$q_{\text{thr}} = W_{\text{pump}} \tau_{\text{del}}; \quad (17)$$

where  $\delta = p_{\text{CO}}/p_{\text{N}_2}$ ;  $h\nu_{00^1}$  is the excitation energy of the upper laser level;  $W_{\text{pump}}$ , specific pump power;  $\gamma$ , fraction of the pump energy fed directly to the upper laser level and to the  $\text{N}_2$  vibrational levels (pump efficiency);  $\gamma_{10^0}$ , efficiency of excitation of the lower laser level;  $\sigma$ , stimulated-emission cross section;  $\alpha_{\text{thr}}$ , threshold value of the gain;  $N_{10^0}$ , population of the lower laser level;  $N_0$ , concentration of the  $\text{CO}_2$  molecules in the mixture;  $\tau_{10^0}$ ,  $\tau_{01^0}$ , and  $\tau_{00^1}$ , lifetimes of the corresponding levels of the  $\text{CO}_2$  molecules;  $R$ , reflection coefficient of the output mirror.

Such parameters as  $\sigma$  and  $N_{10^0}$  cannot change noticeably when small amounts of hydrogen are added to the  $\text{CO}_2:\text{N}_2$  mixture; the value of  $W_{\text{pump}}$  at fixed excitation conditions, as already noted, likewise remains unchanged when the  $\text{H}_2$  content is increased by approximately up to 20%. Therefore, the observed dependences of the lasing characteristics on the hydrogen concentration can be due only to a change in the lifetimes of the upper and lower levels and in the pumping efficiency. At weak excitation, when  $W_{\text{pump}} \geq W_{\text{thr}} = (h\nu_{00^1}/\gamma\tau_{00^1})(\alpha_{\text{thr}}/\sigma + N_{10^0})$  and the nonequilibrium population of the lower laser level can be neglected, an increase of the hydrogen concentration in the  $\text{CO}_2:\text{N}_2:\text{H}_2$  mixture at specified  $W_{\text{pump}}$  and  $\tau_{\text{pump}}$  on account of the decrease in the lifetime of the upper laser level should lead to an increase in the lasing delay time, to an increase of  $W_{\text{thr}}$  and  $q_{\text{thr}}$ , and to a corresponding decrease of the efficiency and of  $q_{\text{em}}$ , as is observed in experiment (see Figs. 15a and 16). As follows from (14), the increase of  $\tau_{\text{del}}$  with increasing  $\text{H}_2$  content, which is observed at  $W_{\text{pump}} \gg W_{\text{thr}}$ , is due mainly to the decreased pumping efficiency. The cause of the decrease of the  $\gamma$  is obvious: since hydrogen has a large cross section for vibrational excitation in the same electron energy region in which the vibrational levels of  $\text{N}_2$  and the level  $00^1$   $\text{CO}_2$

TABLE 5

E/p, kV/ cm · atm	CO <sub>2</sub> :N <sub>2</sub> :H <sub>2</sub>			
	1:2:0	1:2:0,06	1:2:0,125	1:2:0,25
	$\gamma$ (expt)			
~3	0,37	0,33	0,27	0,2
~4	0,5	0,45	0,4	0,34

TABLE 6

Lasing characteristics	CO <sub>2</sub> :N <sub>2</sub> :H <sub>2</sub>								CO <sub>2</sub> :N <sub>2</sub> :He	
	1:1:10	1:1:0,06	1:1:0,17	1:1:1	1:2:0	1:2:0,06	1:2:0,25	1:2:0,5	1:1:3	1:2:3
$P\tau_{10^0}$ , atm · $\mu$ sec	4,3	0,38	0,12	0,05	3,9	0,67	0,2	0,11	0,38	0,64
$\left(1 + \frac{\tau_{10^0}}{\tau_{00^1}}\right)^{-1}$	0,55	0,89	0,91	0,94	0,62	0,87	0,92	0,93	0,97	0,93

Note. The level lifetimes are calculated in accordance with the data of [31, 32, 38].

(16) are effectively excited, it follows that when H<sub>2</sub> is introduced into the mixture, part of the pump energy is consumed in its vibrational excitation [37]. Comparison of the values of  $\tau_{del}$ ,  $q_{thr}$ , and  $\eta$  measured in the long-pulse regime and calculated with the aid of (14)–(17) has shown that the pumping efficiency decreases by 10–30% when the H<sub>2</sub> content in the mixture is as low as 2–8%, and the decrease of  $\gamma$  is more noticeable the smaller the reduced field intensity (see Table 5).

The decrease of  $\tau_{00^1}$  and  $\gamma$  explains, obviously, the decrease, observed in [34], of the weak-signal gain and of the lifetime of the inversion in the EB amplifier when a small amount of H<sub>2</sub> is added to the CO<sub>2</sub>:N<sub>2</sub> working mixture at relatively low pump energies. At high excitation powers, when the population of the lower laser level becomes substantial, the decisive role in the temporal and energy characteristics of the CO<sub>2</sub> laser is assumed by the rate of depletion of the O1<sup>10</sup> level, through which energy relaxes from the 10<sup>0</sup> level. The effect of adding H<sub>2</sub> on the EB laser parameters depends in this case on the relation between the "useful" decrease of the quantity  $\tau_{10^0}$  and the "harmful" decrease of  $\tau_{00^1}$  and  $\gamma$ . At  $W_{pump} \gg W_{thr}$  and  $q_{pump} \gg q_{thr}$  the increase of the H<sub>2</sub> content in the CO<sub>2</sub>:N<sub>2</sub>:N<sub>2</sub> mixture first causes an increase in the specific energy output and in the efficiency (since the quantity  $\tau_{10^0}/\tau_{00^1}$  decreases sharply already at low concentrations of H<sub>2</sub> (see Table 6), and the relative decrease of  $\gamma$  is approximately proportional to the H<sub>2</sub> concentration), but after the H<sub>2</sub> content is increased above a certain optimal value, a noticeable decrease of  $q_{em}$  sets in because of the increase of the threshold and of the decrease of  $\gamma$ .

At low values of E/p, the rates of population of the upper and lower laser levels are comparable [39, 17] and a high pump power is necessary to produce lasing. The lasing delay time depends in this case substantially on the rate of energy relaxation from the 10<sup>0</sup> level. The decrease of  $\tau_{del}$  with increasing H<sub>2</sub> content in the CO<sub>2</sub>:N<sub>2</sub>:H<sub>2</sub> mixture, observed in a wide range of hydrogen concentrations in the case of high-power pumping and  $E/p \lesssim 2$  kV/cm · atm (see Fig. 15b), is apparently due to the corresponding decrease of N<sub>10<sup>0</sup></sub>. It is clear that in the strong-pumping regime the optimal concentration of H<sub>2</sub> should be higher the higher the power and the initial efficiency of the pumping (at a fixed duration of the excitation) and the shorter the pump pulse (at a fixed energy input).

This conclusion is confirmed both by relations (14)–(17) and by experiment: in the long-pulse regime the increase of the pump power at constant field intensity in the discharge gap and at a fixed excitation-pulse duration leads to an increase of the optimal H<sub>2</sub> concentration (Fig. 17), and on going over to short pulses, the optimal hydrogen content increases sharply together with the pump power (see Tables 2 and 3). The increase in the rate of depopulation of the lower laser level following the addition of H<sub>2</sub> into the CO<sub>2</sub>:N<sub>2</sub> mixture leads, in the



strong-pumping regime, to an increase in the lifetime of the inversion in the EB CO<sub>2</sub> amplifier [34], and to a certain increase of the emission pulse duration in the lasing regime.

The experiments performed lead to the following conclusions.

1. In the case of short EB CO<sub>2</sub> laser excitation pulses (at  $W_{\text{pump}} \gg W_{\text{thr}}$ ), it is beneficial to use  $q_{\text{pump}} \gg q_{\text{thr}}$  and  $\tau_{\text{pump}} \lesssim \tau_{00^{\circ}1}$  as the working mixture in order to attain high values of the gain (in an amplifier) and of the emission energy (in a laser). In this regime, hydrogen-containing mixtures are not inferior with respect to lasing efficiency to CO<sub>2</sub>:N<sub>2</sub>:He mixture, and are noticeably superior with respect to the specific energy output.

2. In the quasistationary regime of the EB CO<sub>2</sub> laser ( $W_{\text{pump}} \gg W_{\text{thr}}$ ,  $\tau_{\text{pump}} \gg \tau_{00^{\circ}1}$ ), given the parameters of the ionization source, the use of CO<sub>2</sub>:N<sub>2</sub> mixtures with small (1-3%) additions of hydrogen ensures practically the same output parameters of the EB laser as when CO<sub>2</sub>:N<sub>2</sub>:He mixtures are used (this is also attested by the results of [35]). Since the cost of CO<sub>2</sub>:N<sub>2</sub>:He mixtures are lower by hundreds of times than those of mixtures with helium, they should be employed if the gas consumption is high.

3. In contrast to the TEA CO<sub>2</sub> lasers, in which the improvement of the energy parameters following introduction of a small amount of H<sub>2</sub> into the working mixture CO<sub>2</sub>:N<sub>2</sub>:He is due to the improvement of the discharge characteristics [40, 41], the dependence of the output parameters of EB CO<sub>2</sub> lasers on the hydrogen concentration in the mixture is determined only by the corresponding change in the lifetimes of the laser levels and of the pumping efficiency.

4. Calculations of the lasing characteristics of EB lasers using the CO<sub>2</sub>:N<sub>2</sub>:H<sub>2</sub> mixture, performed in [36], lead to results that are patently too high.

The authors thank A. N. Lobanov and B. M. Urin for a discussion of the results.

#### LITERATURE CITED

1. N. G. Basov, É. M. Belenov, V. A. Danilychev, A. A. Ionin, I. B. Kovsh, and A. F. Suchkov, Zh. Tekh. Fiz., 42, 2540-2549 (1972).
2. N. G. Basov, É. M. Belenov, V. A. Danilychev, O. M. Kerimov, I. B. Kovsh, A. S. Podsozonnii, and A. F. Suchkov, Zh. Eksp. Teor. Fiz., 64, 108-121 (1973).
3. N. G. Basov, V. A. Danilychev, A. A. Ionin, I. B. Kovsh, and V. A. Sobolev, Zh. Tekh. Fiz., 43, 2350 (1973).
4. N. G. Basov, V. A. Danilychev, A. A. Ionin, I. B. Kovsh, V. A. Sobolev, A. F. Suchkov, and B. M. Urin, Kvantovaya Elektron. (Moscow), 1, 2529-2531 (1974).
5. N. G. Basov, V. A. Danilychev, A. A. Ionin, I. B. Kovsh, V. A. Sobolev, A. F. Suchkov, and B. M. Urin, Kvantovaya Elektron. (Moscow), 2, 2458-2467 (1975).
6. T. F. Stratton, G. F. Erickson, C. P. Fenstermacher, and E. D. Zwickard, IEEE J. Quantum Electron., QE-9, 157 (1977).
7. C. Cason, G. J. Dezenberg, and R. T. Huff, Appl. Phys. Lett., 23, 110-111 (1973).
8. J. M. Hoffman, F. W. Bingham, and J. B. Moreno, J. Appl. Phys., 45, 1798-1805 (1974).
9. Yu. I. Bychkov, Yu. A. Kurbatov, and V. V. Savin, Zh. Tekh. Fiz., 44, 803-807 (1974).
10. G. G. Dolgov-Savel'ev, I. D. Kononov, I. A. Leont'ev, V. G. Lyakishev, V. K. Orlov, S. N. Telepin, and N. V. Cheburkin, Kvantovaya Elektron. (Moscow), 2, 214-216 (1975).
11. A. M. Orishin, A. G. Ponomarenko, V. G. Posukh, R. I. Soloukhin, and S. P. Shalamov, Pis'ma Zh. Tekh. Fiz., 3, 39-43 (1977).
12. V. A. Danilychev, O. M. Kerimov, and I. B. Kovsh, High-Pressure Molecular Lasers [in Russian], VINITI, Moscow (1977).
13. A. F. Suchkov and B. M. Urin, FIAN Preprint No. 117, Moscow (1974).
14. A. R. Davies, K. Smith, and R. M. Thomson, J. Appl. Phys., 47, 2037-2043 (1976).
15. I. B. Kovsh, Candidate's Dissertation, FIAN, Moscow (1975).
16. E. W. McDaniel, Collision Phenomena in Ionized Gases, Wiley, New York (1964).
17. A. N. Lobanov and A. F. Suchkov, Kvantovaya Elektron. (Moscow), 1, 1527-1536 (1974).
18. R. C. Smith, Appl. Phys. Lett., 25, 292-295 (1974).
19. R. C. Smith, Appl. Phys. Lett., 20, 56-59 (1972).
20. N. G. Basov, V. A. Danilychev, A. A. Ionin, I. B. Kovsh, V. A. Sobolev, et al., FIAN Report, Moscow (1979).
21. A. S. Biryukov, V. K. Konyukhov, A. I. Lukovnikov, and R. I. Serikov, Zh. Eksp. Teor. Fiz., 66, 1248-1257 (1974).
22. M. C. Fowler, J. Appl. Phys., 43, 3480-3486 (1972).

23. R. Fly and T. K. McCubbin, Jr., *Appl. Opt.*, 9, 1230-1235 (1970).
24. T. K. McCubbin, Jr. and T. R. Mooney, *J. Quantum Spectrosc. Radiat. Transfer*, 8, 1255-1263 (1968).
25. R. R. Patty, E. R. Muring, and J. A. Gardner, *Appl. Opt.*, 7, 2241-2250 (1968).
26. S. D. Rockwood, G. H. Canavau, and W. A. Proctor, *IEEE J. Quantum Electron.*, QE-9, 154-161 (1973).
27. V. P. Tychinskii, *Usp. Fiz. Nauk*, 91, 389-424 (1967).
28. N. N. Sobolev and V. V. Sokovikov, *Usp. Fiz. Nauk*, 91, 425-452 (1967).
29. O. R. Wood, *Proc. IEEE*, 62, 355-401 (1974).
30. F. S. Aslibekyan, I. K. Babaev, V. A. Danilychev, V. T. Dauge, I. B. Kovsh, V. K. Orlov, et al., *Laser Welding of a Block of Ground Gears of the 16N20 Lathe [in Russian]*, Sci.-Tech. Report, Moscow (1977).
31. R. L. Taylor and S. Bitterman, *Rev. Mod. Phys.*, 41, 26-55 (1969).
32. T. G. Winter, *J. Chem. Phys.*, 38, 2761-2764 (1963).
33. C. B. Moore, R. E. Wood, Bei-Lok Hu, and J. T. Jardley, *J. Chem. Phys.*, 46, 4222-4225 (1967).
34. C. H. H. Carmichael, R. K. Garthworthy, and L. E. S. Mattias, *Appl. Phys. Lett.*, 24, 608-610 (1974).
35. D. H. Douglas-Hamilton, R. M. Feinberg, and R. S. Lowder, *J. Appl. Phys.*, 46, 3566-3575 (1975).
36. L. V. Dubovoi, V. A. Zaitsev, and V. P. Poponin, *Pis'ma Zh. Tekh. Fiz.*, 1, 411-415 (1975).
37. N. V. Karlov, Yu. B. Konev, I. V. Kochetov, and V. G. Pevgov, *FIAN Preprint No. 91*, Moscow, (1976).
38. J. W. L. Lewis and K. P. Lee, *J. Acoust. Soc. Am.*, 38, 813-819 (1965).
39. J. J. Lowke, A. V. Phelps, and B. W. Irwin, *J. Appl. Phys.*, 44 (1973).
40. T. F. Deutsch, *Appl. Phys. Lett.*, 20, 315-318 (1972).
41. A. L. S. Smith, T. H. Bett, and P. G. Browne, *IEEE J. Quantum Electron.*, QE-11, 335-337 (1975).